Drought Response to Air Temperature Change over China on the Centennial Scale

CHEN Huo-Po[1,2] and SUN Jian-Qi[1]

[1] *Nansen-Zhu International Research Centre, Institute of Atmospheric Physics, Chinese Academy of Sciences, Beijing 100029, China*
[2] *Collaborative Innovation Center on Forecast and Evaluation of Meteorological Disasters, Nanjing University of Information Science & Technology, Nanjing 210044, China*

Received 24 November 2014; revised 26 December 2014; accepted 12 January 2015; published 16 May 2015

Abstract Climate data from the Climatic Research Unit (CRU) for the period 1901–2013 are used to investigate the drought response to air temperature change over China on the centennial scale. Drought is observed to have increased evidently across China, except for some regions in eastern China. This increase is much stronger in northern China compared to southern China, especially in Northwest and North China. These change characteristics of drought are closely associated with air temperature change, with the severe droughts in the major drought episodes of the last century generally coinciding with higher temperatures. The significantly increasing trend of drought in China based on observations only appears when considering the effects of air temperature change, which can explain ~49% of droughts in observations and 30%–65% of droughts in Coupled Model Intercomparison Project Phase 5 (CMIP5) model simulations. Furthermore, the response of drought to air temperature change generally increases as the drought time scale increases. Furthermore, drought shows relatively high sensitivity in spring and early summer in China on the centennial scale.

Keywords: drought, air temperature, response, centennial scale, China

Citation: Chen, H.-P., and J.-Q. Sun, 2015: Drought response to air temperature change over China on the centennial scale, *Atmos. Oceanic Sci. Lett.*, **8**, 113–119, doi:10.3878/AOSL20140089.

1 Introduction

Drought is one of the most damaging natural hazards affecting the regions of China, causing destructive impacts on agriculture, industry, water resources, and ecosystems (Ma and Fu, 2006; Wang et al., 2011; Liu and Jiang, 2014). Many studies have documented that there has been an increase in drought severity in recent decades in China (e.g., Zou et al., 2005; Xin et al., 2006; Zhai et al., 2010) and the dry region is reported to be increasing by ~3.72% per decade (Yu et al., 2014), mainly associated with the climate variability of precipitation (e.g., Lu et al., 2011).

The global warming process has attracted increased attention from government bodies, the scientific community, and the public (e.g., Intergovernmental Panel on Climate Change (IPCC), 2013). There is consensus that the rise in air temperature plays an important role in increasing drought severity (Vicente-Serrano et al., 2010). The higher temperatures increase the water pressure deficit, raising the atmospheric evaporative demand and causing more frequent and severe droughts (Dai, 2011; Wang et al., 2012). However, the consequences of the recent air temperature increase for drought severity are not well understood due to some problems with the quantification of drought (Redmond, 2002) and data uncertainty (Trenberth et al., 2014). For example, recent studies show almost contradictory results in their analysis of the impact of temperature rise on drought severity worldwide, due to the different methods used for estimating the evaporative demand of the atmosphere (Dai, 2012; Sheffield et al., 2012). Furthermore, the uncertainty appears greater when analyses focus on the regional scale. The drought severity of the Iberian Peninsula has been reported to have increased during the past five decades, as a consequence of climate warming (Vicente-Serrano et al., 2014). However, some studies also indicate no effect of temperature rise on drought through increased evaporation for some regions around world (McVicar et al., 2012).

For China, relative to global warming, the air temperature increase is happening at a much faster rate, resulting in more frequent and severe droughts in the country during the past five decades (Yu et al., 2014). Extending back to the 20th century, instrumental observations show the air temperature to have increased by ~1.5°C in the last century (Cao et al., 2013). But what about the response of drought severity to air temperature change during this period? Thus far, this issue has not been investigated. Accordingly, the aim of the present study is to investigate the long-term trends of drought in China and its associated responses to air temperature change on a centennial scale. The results not only provide robust validations of previous work that mainly focused on the past five decades, but also form a scientific basis for the enhancing dry conditions resulting from continuous warming in the future.

2 Data and methods

To quantify drought, we use the standardized precipitation evapotranspiration index (SPEI) (Vicente-Serrano et al., 2010), which is based on the water balance between precipitation and evapotranspiration, and the standardized precipitation index (SPI) (McKee et al., 1993), which is only based on precipitation data. The SPEI and the SPI

Corresponding author: CHEN Huo-Po, chenhuopo@mail.iap.ac.cn

are calculated on different time scales of 1–24 months and the drought characteristics are mainly investigated using the 12-month scale. The droughts here are defined as the SPEI/SPI less than the threshold of −1.28. This threshold is selected according to its probability distribution function and it is equivalent to the 10% chance of the drought event having happened. The linear regression method is used to detect the change trends of drought on different time scales for China.

The monthly precipitation, air temperature, and potential evapotranspiration from the Climatic Research Unit (CRU) for the period 1901–2013 (referred to as CRU TS3.22; Harris et al., 2014) are used to calculate the SPEI/SPI. Potential evapotranspiration has only recently been included in the CRU dataset and is calculated from a variant of the Penman-Monteith formula using mean temperature, maximum and minimum temperatures, vapor pressure, and cloud cover. To better understand the drought response to the air temperature change at the centennial scale, the simulated monthly precipitation and temperature from Coupled Model Intercomparison Project Phase 5 (CMIP5) models (Table 1) are also used for the period 1901–2005. The potential evapotranspiration for the models is calculated using the Thornthwaite method (Thornthwaite, 1948) due to the limitations of the available datasets.

Table 1 List of 35 Coupled Model Intercomparison Project Phase 5 (CMIP5) models used in this study.

Label	Model ID	Model full name	Nation	Atmospheric component resolution (latitude×longitude)
1	ACCESS1-0	Australian Community Climate and Earth System Simulator coupled model (version 1.0)	Australia	1.25° × 1.875°
2	BCC-CSM1.1m	Beijing Climate Center Climate System Model (version 1.1m)	China	1.112° × 1.125°
3	BCC-CSM1.1	Beijing Climate Center Climate System Model (version 1.1)	China	2.784° × 2.8125°
4	BNU-ESM	Beijing Normal University Earth System Model	China	2.784° × 2.8125°
5	CanESM2	Second generation Canadian Earth System Model	Canada	2.784° × 2.8125°
6	CCSM4	Community Climate System Model (version 4.0)	USA	0.942° × 1.25°
7	CESM1-BGC	Community Earth System Model version 1 (CESM1), Biogeochemistry cycling model	USA	0.942° × 1.25°
8	CESM1-CAM5	CESM1, Community Atmospheric Model version 5	USA	0.9° × 1.25°
9	CESM1-FASTCHEM	Community Earth System Model with FASTCHEM	USA	0.942° × 1.25°
10	CESM1-WACCM	CESM1, Whole Atmosphere Community Climate Model	USA	1.875° × 2.5°
11	CMCC-CESM	CMCC (Centro Euro-Mediterraneo per I Cambiamenti Climatici) Carbon Earth System Model	Europe	3.75° × 3.7°
12	CMCC-CM	CMCC Climate Model	Europe	0.75° × 0.75°
13	CMCC-CMS	CMCC Climate Model with a resolved Stratosphere	Europe	1.861° × 1.875°
14	CNRM-CM5	Centre National de Recherches Météorologiques (Climate Model version 5)	France	1.397° × 1.406°
15	CSIRO-MK3.6.0	Commonwealth Scientific and Industrial Research Organisation (Mark 3.6.0)	Australia	1.861° × 1.875°
16	FGOALS-g2	Flexible Global Ocean-Atmosphere-Land System Model, Grid Version 2	China	2.8125° × 2.8125°
17	FGOALS2-s	Flexible Global Ocean-Atmosphere-Land System Model, Spectral Version 2	China	1.7° × 2.8°
18	FIO-ESM	First Institute of Oceanography-Earth System Model	China	2.8° × 2.8°
19	GFDL-CM2p1	Coupled Climate Model version 2.1 of Geophysical Fluid Dynamics Laboratory	USA	2.0225° × 2.5°
20	GFDL-ESM2G	Earth System Model of Geophysical Fluid Dynamics Laboratory (Generalized Ocean Layer Dynamics, GOLD)	USA	2.0225° × 2.5°
21	GFDL-ESM2M	Earth System Model of Geophysical Fluid Dynamics Laboratory (Modular Ocean Model Version 4.1, MOM4.1)	USA	2.0225° × 2.5°
22	GISS-E2-H	E2 version of the Goddard Institute for Space Studies Climate Model (ModelE/Hycom)	USA	2.0225° × 2.5 º
23	GISS-E2-H-CC	E2 version of the Goddard Institute for Space Studies Climate Model-Carbon Cycle (ModelE/Hycom)	USA	2.0225° × 2.5 º
24	HadCM3	Hadley Climate Model 3	UK	2.5° × 3.75°
25	INMCM4	Version 4 of the Institute of Numerical Mathematics Climate Model	Russia	1.5° × 2°
26	IPSL-CM5A-MR	Earth System Model of the Institut Pierre Simon Laplace: Medium Resolution	France	1.268°× 2.5°
27	IPSL-CM5A-LR	Earth System Model of the Institut Pierre Simon Laplace: Low Resolution	France	1.895° × 3.75°
28	IPSL-CM5B-LR	Earth System Model of the Institut Pierre Simon Laplace: Low Resolution	France	1.895° × 3.75 º
29	MPI-ESM-LR	Earth System Model of Max-Planck-Institut für Meteorologie: Low Resolution	Germany	1.861° × 1.875°
30	MPI-ESM-MR	Earth System Model of Max-Planck-Institut für Meteorologie: Medium Resolution	Germany	1.861° × 1.875°
31	MPI-ESM-P	Earth System Model of Max-Planck-Institut für Meteorologie: Low resolution grid and paleo mode	Germany	1.9° × 1.9°
32	MIROC-ESM	Earth System Model of MIROC	Japan	2.784° × 2.8125°
33	MIROC-ESM-CHEM	An atmospheric chemistry coupled version of MIROC-ESM	Japan	2.784° × 2.8125°
34	NorESM1-M	Norwegian Climate Center's Earth System Model	Norway	1.895° × 2.5°
35	NorESM1-ME	Norwegian Climate Center's Earth System Model including prognostic biogeochemical cycling	Norway	1.895° × 2.5°

3 Results

Figure 1 show plots of the changes in drought characteristics for mainland China in the period 1902–2013 based on the 12-month SPEI. Spatially, the evolution of drought across China predominantly increases (more drought), although some regions in eastern China show a decreasing trend (Fig. 1a). The trend statistics on the centennial scale of increasing drought in Northeast, North, Central, and Southwest China, and decreasing drought in eastern China, agree well with the changes during the past 50 years[①]. However, the drought changes in Northwest China are quite different on the centennial scale in comparison to the changes in recent decades. From the late 1980s, the precipitation over Northwest China is reported to have significantly increased and its dry condition mitigated (Chen et al., 2012). However, the dry condition is shown to persistently deteriorate on the centennial scale, and the region of Northwest China is dominated by the largest increasing-trend statistics across China.

Figure 1b presents the spatial patterns of the long-term trends of potential evapotranspiration for China in the last century, indicating a general increase across the country. The increased potential evapotranspiration probably resulted in an increase in actual evaporation, which would have directly related to the increase in surface heating and then aggravated the dry condition regionally (Trenberth et al., 2014). The spatial patterns of the potential evapotranspiration changes on the centennial scale show strong similarities with the drought changes in China. Increasing numbers of droughts are generally associated with a large increase of potential evapotranspiration, particularly in the northern regions of China. In southern China, the increasing trend of drought is relatively weaker or even decreases, although a strong increase is observed for the potential evapotranspiration over these regions. This implies that the response of drought to air temperature changes varies regionally across China. Relatively strong responses to temperature changes are found over northern China and relatively weak responses over southern China. This spatial inhomogeneity in the response is partially associated with the local variation in total precipitation amounts. There is sufficient precipitation in southern China to meet the high water demand of potential evapotranspiration, resulting in relatively weak drought responses to air temperature change. However, this situation is reversed in northern China, where relatively strong responses to air temperature changes can be observed. These results are also true when the analysis is performed for the last 50 years[①].

The temporal variations in drought frequency and area anomalies for China in the period 1902–2013 are also shown in Fig. 1. Major drought episodes in China are recorded for the 1940s, 1980s, and 2000s (Fig. 1c). The surface area affected by drought is also observed to increase over the same time period (Fig. 1d). For the period 1902–2013, the trend patterns indicate that drought over China increased significantly, with trend statistics of 0.1 month per decade for drought frequency and 1.3% per decade for drought area. In comparison to the air temperature change, there is substantial agreement between the drought and temperature anomalies. The major drought episodes of the last century are generally dominated by higher temperatures. Nevertheless, the drought conditions in the last 10 years, which include the warmest years on record since 1850, are the severest for the entire time period in China. This evidence indicates that air temperature is one of the major climatic drivers for drought, and its change plays an important role in determining the occurrence, duration, and severity of drought.

To further understand the drought response to air temperature change in China, the differences between the SPEI and the SPI are investigated. The variation of their differences mainly reflects the impacts of air temperature change on drought because the SPI is calculated based on precipitation only. The corresponding results are shown in Fig. 2. There are some differences between the SPEI and the SPI time series for China, and the droughts represented by the SPI show relatively weaker or even no trends on the centennial scale (Figs. 2a and 2d). The droughts over the major drought episodes are also much weaker when just the effect of precipitation is considered, in comparison to the SPEI. For the droughts in the last 10 years in particular, they are the severest in the past 100 years according to the SPEI; however, the results based on the SPI indicate below-normal levels of drought both in terms of drought frequency and drought area anomalies. The trends in the annual differences for drought frequency (Fig. 2b) and area (Fig. 2e) between the two indices (i.e., SPEI minus SPI) show a dominant upward trend, indicating a positive impact of air temperature change on drought. This impact is highly evident for the several major droughts with higher temperature records in the past 100 years. Nevertheless, the result from the SPEI also indicates the occurrence of more intense drought events relative to the SPI (figure not shown). We compute the correlations between the differences from the two indices and the air temperature change in China for the period 1902–2013, and find a value of 0.74 for drought frequency and 0.71 for drought area. This implies that there is an equivalent role in determining drought in China between precipitation and temperature on the centennial scale, provided no consideration of their nonlinear interactions or influences from other factors (e.g., wind speed, radiation, humidity, and surface characteristics) on potential evapotranspiration. Approximately 49% of the droughts can be simply explained by potential evapotranspiration change; that is, mainly by air temperature change.

Spatially, the linear trends of drought frequency difference between the SPEI and the SPI (Fig. 2c) indicate an increasing trend across China, with relatively large change magnitudes in northern China and relatively small change magnitudes in southern China. Thus, we can conclude that drought shows a relatively strong response to air temperature change in northern China and a relatively

[①]Chen, H. P., and J. Q. Sun, 2014: Changes in drought characteristics over China using the standardized precipitation evapotranspiration index, submitted to *J. Climate*.

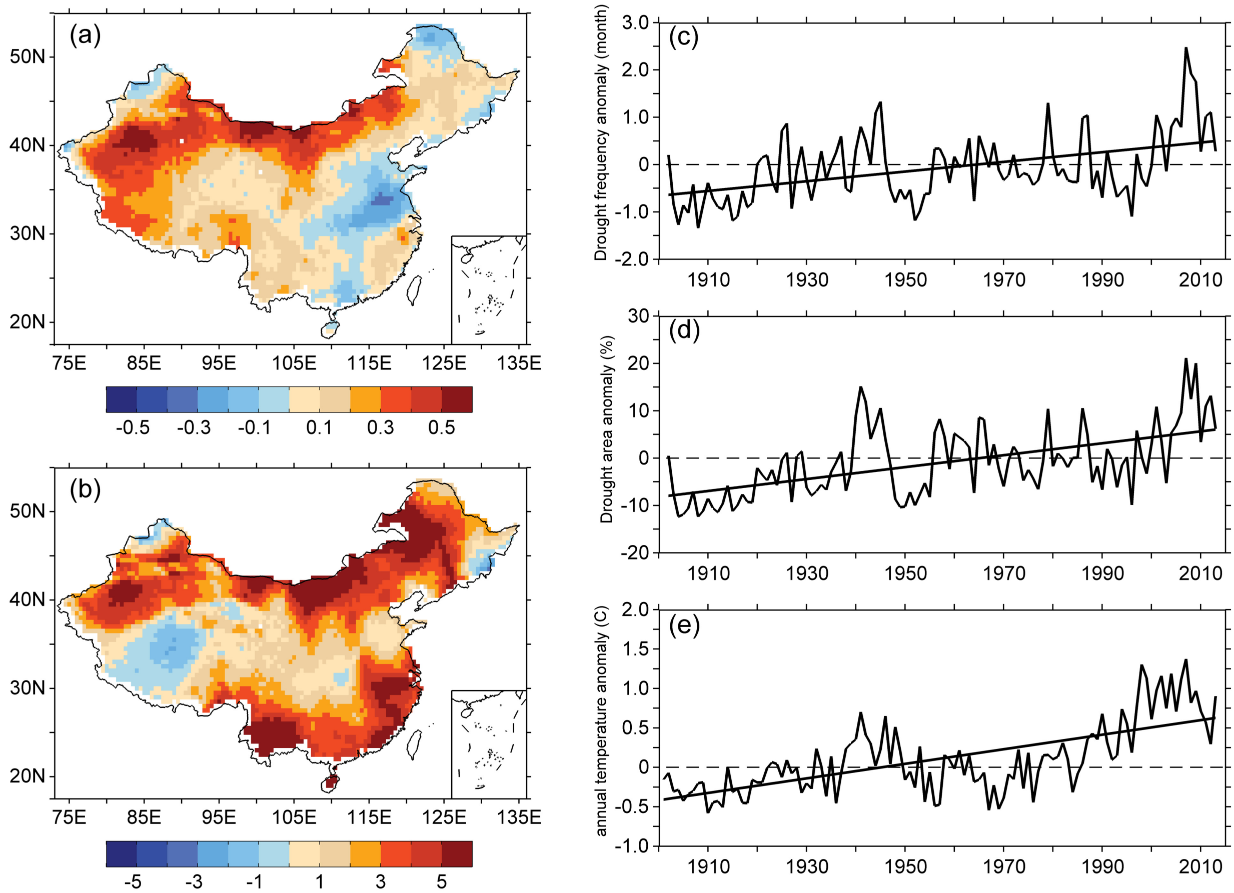

Figure 1 Plots of drought change characteristics in China for the period 1902–2013: (a) spatial patterns of annual drought frequency trends (months per decade); (b) as in (a) but for the long-term trends of potential evapotranspiration in China (mm per decade); (c) temporal evolution of the regional annual drought frequency for China from 1902 to 2013; (d) as in (c) but for the temporal evolution of the drought area anomaly; (e) evolution of the regional annual air temperature anomaly in China. The drought frequency and area are selected based on an SPEI threshold of −1.28, which corresponds to 10% of events according to the probability distribution function. The anomalies are estimated with respect to the period 1961–1990.

weak response in southern China as mentioned above. Certainly, this difference in drought response from north to south is also closely associated with the different change magnitudes of air temperature, with a relatively large increase in northern China and a relatively small increase in southern China.

The aforementioned analyses are mainly implemented using the SPEI/SPI on the 12-month time scale. But what about the response of drought to air temperature change on other time scales? Figure 2f shows plots of the linear trends for the drought area difference between the SPEI and the SPI for each month at time scales of 1–24 months. Clearly, the drought responses to air temperature change vary with season and with time scale. Relatively strong responses of drought can be observed in spring and early summer, which are nearly independent of the time scale of the SPEI/SPI, while relatively weak responses are apparent in other months, especially from July to October on the 1–3 month time scales. This indicates a high sensitivity of drought to air temperature change in spring and early summer in China. Furthermore, the response of drought generally increases as the drought time scale increases.

As shown by recent climate model simulations, similar results can be obtained as those based on observational records. Figure 3 presents the simulated linear trends for the annual drought area difference in China between the SPEI and the SPI at the time scales of 1–24 months for the period 1903–2005 from 35 CMIP5 models. Evidently, all the models indicate positive responses of drought to air temperature change in China on the centennial scale, and the magnitudes of the responses increase as the time scale increases. However, the response magnitudes vary from model to model, with relatively strong responses for FGOALS2-s, FIO-ESM, IPSL-CM5A-LR, and CESM1-WACCM, and relatively weak responses for MIROC-ESM, GISS-E2-H, CSIRO-MK3.6.0, and CMCC-CESM. The multi-model ensemble (MME) results from all the models are also shown in Fig. 3. Positive trends can be observed for all time scales, and are relatively stronger than the observational records. We also calculate the correlation coefficients between the annual drought area differences (i.e., SPEI minus SPI) and the air temperature changes in China from the historical simulations of the models, and find them to range from 0.55 to 0.81. Thus, based on the model simulations, air temperature change can be considered to explain 30%–65% of drought on the centennial scale, which is quite similar to the results based

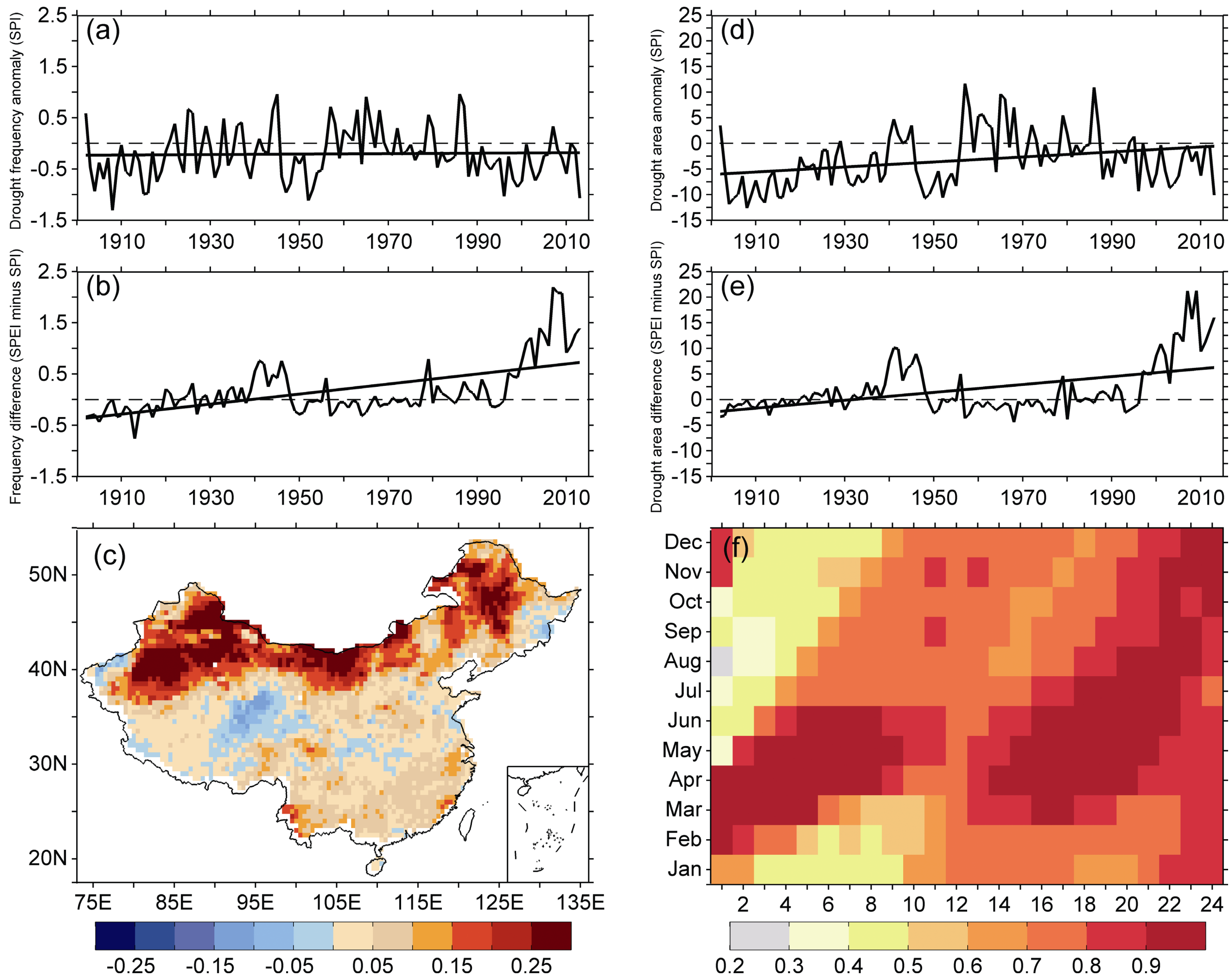

Figure 2 (a) Evolution of the regional annual drought frequency anomaly for the period 1902–2013 based on the SPI. (b) Difference between the SPEI and the SPI with respect to annual drought frequency. (c) Spatial distribution of the linear trends for the difference of annual drought frequency between the SPEI and the SPI from 1902 to 2013 (months per decade). (d, e) The corresponding evolutions of the percentages of drought areas in China as in (a, b), respectively. (f) Plots of the linear trends for the drought area difference between the SPEI and the SPI for each month at time scales of 1–24 months (% per decade). The drought frequency and area are selected based on an SPEI/SPI threshold of −1.28 and their anomalies are estimated with respect to 1961–1990.

on observations.

4 Conclusions

Previous studies have documented that China has experienced more frequent and severe droughts in the past five decades[①] (e.g., Yu et al., 2014). These trends are also found to be true when the period considered stretches back to the year 1901, as determined by the analyses in the present study based on the latest version of the CRU dataset. The regions of China have been subject to an increase in aridity on the centennial scale, caused by a significant rise in air temperature (~1.5°C annually) coupled with a weak increase in precipitation (~5.2%). Spatially, drought in China also varies from region to region, with a relatively large increase in northern China, especially Northwest and North China, a relatively small increase in southern China, and even a decrease in some regions of eastern China.

The drought variability is mainly controlled by precipitation, but the drought severity can be exacerbated by the greater evaporative demand of the atmosphere, which increased by ~4.2% annually in the period 1901–2013. Because of the complexity of drought occurrence, it is challenging to isolate the effects on drought of precipitation and air temperature change. The present study attempts to examine the response of drought to air temperature change by simply assuming a linear relationship among their climatic drivers. The recorded increase in drought cannot be captured well by the SPI, but the trends are observed to evidently increase when the effects of climate warming are considered on the centennial scale. Based on this simple assumption, approximately 49% of the drought variability based on observations, and 30%–65% based on CMIP5 models, can be explained by the air temperature changes. Actually, these values are likely to be relatively smaller than presented in this study, because the potential evapotranspiration estimated by the Penman-Monteith method is also determined by other factors, such as wind speed, radiation, humidity, and surface characteristics (McVicar et al., 2012; Wang and Dickinson, 2012; McAfee, 2013); and their influences on evapotranspiration vary from region to region. For exam-

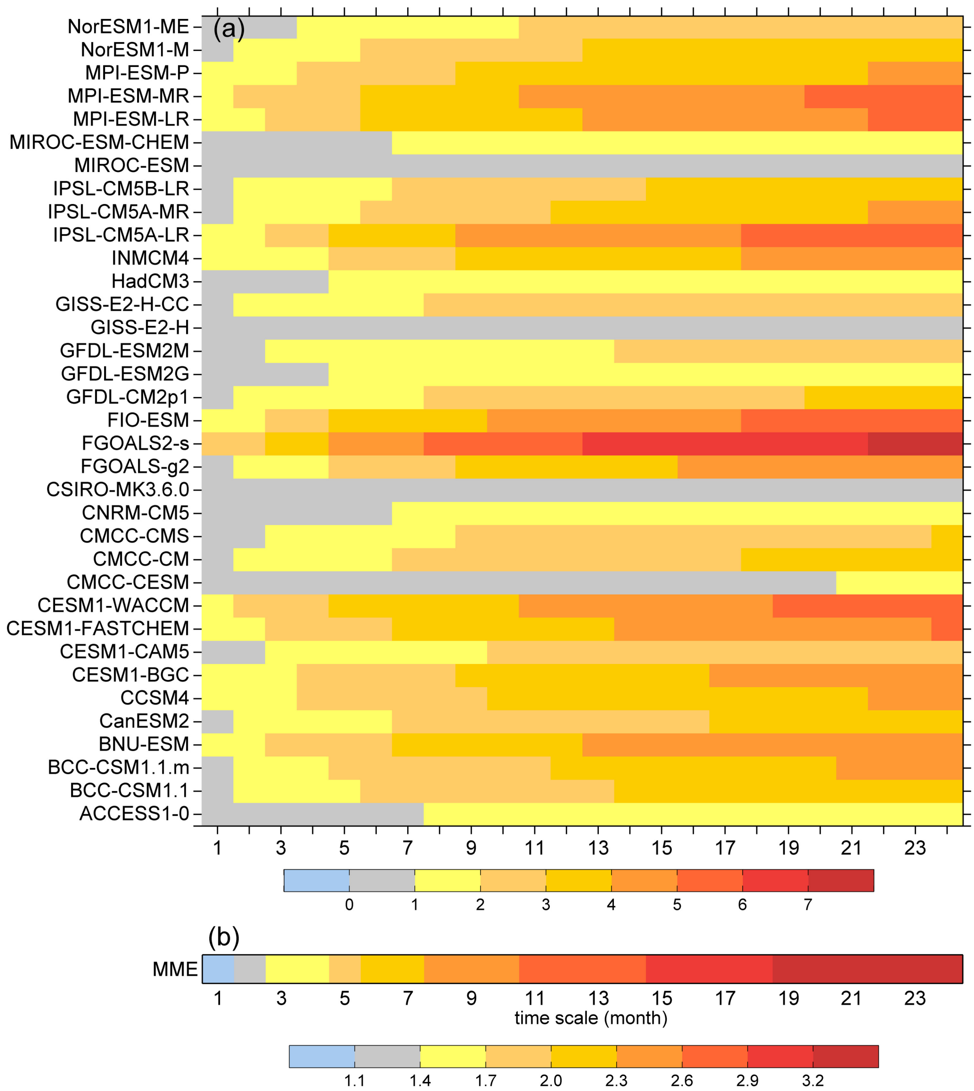

Figure 3 Plots of the simulated linear trends for the annual drought area difference between the SPEI and the SPI at time scales of 1–24 months for the period 1903–2005 from CMIP5 models: (a) CMIP5 models, and (b) multi-model ensemble result. The percentage of drought area is estimated based on the SPEI/SPI being less than −1.28. Units: % per decade.

ple, a relatively greater role of wind change in the evaporation trend can be observed over Australia, USA, and Western Europe, but a relatively smaller role in western Africa, northern South America, South Asia, and East Asia, especially across China (McVicar et al., 2012). Furthermore, their roles are generally relatively weaker than the air temperature changes. Thus, the impacts of these factors have not been isolated from temperature, also due to data limitations. Additionally, results also indicate that the response of drought to air temperature change becomes stronger as the drought time scale increases, and also varies seasonally, with a relatively strong response in spring and early summer in China on the centennial scale.

Acknowledgements. We sincerely appreciate the comments of the two anonymous reviewers, which greatly improved the manuscript. This research was jointly supported by the 'Strategic Priority Research Program—Climate Change: Carbon Budget and Relevant Issues' of the Chinese Academy of Sciences (Grant No. XDA05090306), the National Natural Science Foundation of China (Grant No. 41305061), and the National Basic Research Program of China (Grant No. 2012CB955401).

References

Cao, L., P. Zhao, Z. Yan, et al., 2013: Instrumental temperature series in eastern and central China back to the nineteenth century, *J. Geophys. Res. Atmos.*, **118**, 8197–8207, doi:10.1002/jgrd.50615.

Chen, H. P., J. Q. Sun, and K. Fan, 2012: Possible mechanism for the interdecadal change of Xinjiang summer precipitation, *Chin. J. Geophys.*, **55**(3), 267–274.

Dai, A. G., 2011: Drought under global warming: A review, *Wiley Interdiscip. Rev. Climate Change*, **2**, 45–65.

Dai, A. G., 2012: Increasing drought under global warming in observations and models, *Nature Climate Change*, **3**, 52–58, doi:10.1038/NCLIMATE1633.

Harris, I., P. D. Jones, T. J. Osborn, et al., 2014: Updated high-resolution grids of monthly climatic observations-the CRU TS3.10 Dataset, *Int. J. Climatol.*, **34**, 623–642.

IPCC, 2013: *Climate Change 2013: The Physical Science Basis. Contribution of Working Group I to the Fifth Assessment Report*

I of the Intergovernmental Panel on Climate Change, T. F. Stocker et al. (Eds.), Cambridge University Press, Cambridge and New York, 1535pp.

Liu, K., and D. B. Jiang, 2014: Interdecadal change and cause analysis of extreme summer and winter droughts over China, *Chin. J. Atmos. Sci.* (in Chinese), **38**(2), 309–321.

Lu, X., X. Yang, and S. Li, 2011: Dam not sole cause of Chinese drought, *Nature*, **475**, 174, doi:10.1038/475174c.

Ma, Z. G., and C. B. Fu, 2006: Some evidence of drying trend over northern China from 1951 to 2004, *Chin. Sci. Bull.*, **51**, 2913–2925.

McAfee, S. A., 2013: Methodological differences in projected potential evapotranspiration, *Climate Change*, **120**, 915–930.

McKee, T. B., N. J. Doesken, and J. Kleist, 1993: The relationship of drought frequency and duration to time scales. Preprints, in: *Eight Conference on Applied Climatology*, Amer. Meteor. Soc., Anaheim, CA, 179–184.

McVicar, T. R., M. L. Roderick, R. J. Donohue, et al., 2012: Global review and synthesis of trends in observed terrestrial near surface wind speeds: Implications for evaporation, *J. Hydrol.*, **416–417**, 182–205.

Redmond, K. T., 2002: The depiction of drought, *Bull. Amer. Meteor. Soc.*, **83**, 1143–1147.

Sheffield, J., E. F. Wood, and M. L. Roderick, 2012: Little change in global drought over the past 60 years, *Nature*, **491**, 435–438.

Thornthwaite, C. W., 1948: An approach toward a rational classification of climate, *Geogr. Rev.*, **38**, 55–97.

Trenberth, K. E., A. G. Dai, G. van der Schrier, et al., 2014: Global warming and changes in drought, *Nature Climate Change*, **4**, 17–22, doi:10.1038/NCLIMATE2067.

Vicente-Serrano, S. M., S. Beguería, and J. I. López-Moreno, 2010: A multiscalar drought index sensitive to global warming: The standardized precipitation evapotranspiration index, *J. Climate*, **23**, 1696–1718, doi:10.1175/2009JCLI2909.1.

Vicente-Serrano, S. M., J.-I Lopez-Moreno, S. Beguería, et al., 2014: Evidence of increasing drought severity caused by temperature rise in southern Europe, *Environ. Res. Lett.*, **9**, 1–9.

Wang, A., D. Lettenmaier, and J. Sheffield, 2011: Soil moisture drought in China, 1950–2006, *J. Climate*, **24**, 3257–3271.

Wang, K., and R. E. Dickinson, 2012: A review of global terrestrial evapotranspiration: Observation, modeling, climatology, and climatic variability, *Rev. Geophys.*, **50**, RG2005, doi:10.1029/2011RG000373.

Wang, K., R. E. Dickinson, and S. Liang, 2012: Global atmospheric evaporative demand over land from 1973 to 2008, *J. Climate*, **25**, 8353–8361.

Xin, X., R. Yu, T. Zhou, et al., 2006: Drought in late spring of South China in recent decades, *J. Climate*, **19**, 3197–3206.

Yu, M. X., Q. F. Li, M. J. Hayes, et al., 2014: Are droughts becoming more frequent or severe in China based on the standardized precipitation evapotranspiration index: 1951–2010? *Int. J. Climatol.*, **34**, 545–558, doi:10.1002/joc.3701.

Zhai, J., B. Liu, H. Hartmann, et al., 2010: Dryness/wetness variations in ten large river basins of China during the first 50 years of the 21st century, *Quat. Int.*, **226**, 101–111.

Zou, X., P. Zhai, and Q. Zhang, 2005: Variations in drought over China: 1951–2003, *Geophys. Res. Lett.*, **32**, L04707, doi:10.1029/2004GL021853.